

# Configurational entropy and instability of tachyonic braneworld

Chong Oh Lee\*

*Department of Physics, Kunsan National University, Kunsan 573-701, Republic of Korea*

We consider tachyonic braneworld with a bulk cosmological constant and investigate a configurational entropy of various magnitudes of scale factor. It is found that for a bulk negative/zero cosmological constant, the configurational entropy has a global minimum when the magnitude of scale factor reaches the critical value. This result seems to have intriguing implications such that an accelerated rate of the universe and cosmological inflation rate for radiation/matter domination are able to be determined by such critical value. We also find that the configurational entropy almost monotonically decreases for a bulk positive cosmological constant as the magnitude of scale factor grows up. We find an exact solution of tachyonic braneworld in a bulk de Sitter space. It is shown that such system under scalar perturbations is stable for some constraint relation. Furthermore, we also find that tachyonic braneworld model with a bulk negative/zero cosmological constant is always stable under scalar perturbations.

## I. INTRODUCTION

The D-brane with tachyon condensation [1] has been suggested in search for off-shell structure of string theory. Tachyon dynamics on unstable D-branes was investigated in [2–4] through boundary conformal field theory and effective field theory. In particular, such effective field theory has been extensively applied to inhomogeneous rolling tachyon [5–8], creation of closed string and particle [9, 10] and instability of D-branes of codimension-one [9, 11–13].

A branch of models with bulk scalar fields has been recently suggested in search for tachyonic braneworld scenario with a bulk cosmological constant. It has been found that there is an exact solution for tachyonic braneworld model with/without a bulk cosmological constant [14, 15] and such model is stable under scalar perturbations [15, 16].

The configurational entropy has been suggested in search for the informational entropy [17] and recently applied to the spatially localized energy solutions of nonlinear models [18]. The configurational entropy has used to study instability of a variety of physical systems [18–28].

The paper is organized as follows: in the following section, we will calculate the configurational entropy of tachyon effective theory in case of the Anti-de Sitter (AdS), flat and de Sitter (dS). In the next section, we will explore instability of tachyonic braneworld in the bulk dS space. In the last section we will give our conclusion.

## II. CONFIGURATIONAL ENTROPY

One considers the energy density  $\rho(x)$  as the function of the position  $x$  in  $d$ -dimensional space and the system is spatially localized energy. Its Fourier transforms  $\rho(k)$

is written as

$$\rho(k) = \left(\frac{1}{\sqrt{2\pi}}\right)^d \int \rho(x) e^{-ik \cdot x} d^d x, \quad (2.1)$$

and the modal fraction reads

$$\mathcal{F}(k) = \frac{|\mathcal{P}(k)|^2}{\int |\mathcal{P}(k)|^2 d^d k}, \quad (2.2)$$

which measures the relative weight of a given mode  $k$ . One may define the configurational entropy  $S_c[\mathcal{F}]$  as

$$S_c[\mathcal{F}] = - \sum_{l=1}^n \mathcal{F}_l \ln(\mathcal{F}_l), \quad (2.3)$$

which reduces to

$$S_c[\mathcal{F}] = - \int_{-\infty}^{\infty} \mathcal{G}(k) \ln[\mathcal{G}(k)] d^d k, \quad (2.4)$$

for  $n \rightarrow \infty$ , where  $\mathcal{G}(k) = \mathcal{F}(k)/\mathcal{F}(k)_{\max}$  and the maximum modal fraction  $\mathcal{F}(k)_{\max}$ .

The action for the tachyonic braneworld model is given as

$$A = A_c - A_m, \quad (2.5)$$

where  $A_c$  is the five-dimensional gravity action with the bulk cosmological constant  $\Lambda_5$ ,  $A_m$  is the action of the matter in the bulk,

$$A_c = \int d^5 x \sqrt{-\det(g_{\mu\nu})} \left( \frac{1}{2k_5^2} \mathcal{R} - \Lambda_5 \right), \quad (2.6)$$

$$A_m = \int d^5 x V(T) \sqrt{-\det(g_{\mu\nu} + \partial_\mu T \partial_\nu T)}. \quad (2.7)$$

Here  $k_5$  is the five-dimensional gravitational constant ( $k_5^2 \equiv 8\pi G_5$ ),  $\mathcal{R}$  is the five-dimensional scalar curvature,  $T$  is the tachyon field, and  $V(T)$  is the tachyon potential. The action (2.5) leads to the five-dimensional Einstein equation with the bulk cosmological constant

$$G_{\mu\nu} = -k_5^2 \Lambda_5 g_{\mu\nu} + k_5^2 T_{\mu\nu}. \quad (2.8)$$

The five-dimensional metric ansatz with an induced 3-brane of Friedmann-Robertson-Walker (FRW) background type is given as

$$ds^2 = e^{2f(x)} [-dt^2 + a^2(t)(d\alpha^2 + d\beta^2 + d\gamma^2) + dx^2], \quad (2.9)$$

\* cohlee@gmail.com

where  $e^{2f(x)}$  denotes the warp factor, and  $a(t)$  does the scale factor on the brane. Then, the Einstein tensor  $G_{\mu\nu}$  (2.8) have the nonvanishing components:

$$G_{tt} = \frac{3\dot{a}^2}{a^2} - 3(f'' + 2f'^2), \quad (2.10)$$

$$G_{\alpha\alpha} = G_{\beta\beta} = G_{\gamma\gamma} = -2\ddot{a}a - \dot{a}^2 + 3a^2(f'' + 2f'^2), \quad (2.11)$$

$$G_{xx} = -3\left(\frac{\ddot{a}}{a} + \frac{\dot{a}^2}{a^2}\right) + 6f'^2, \quad (2.12)$$

where the dot and the prime denote time and spatial derivative, respectively. After taking  $a(t) = e^{Ht}$ , the matter field equations are given as

$$\begin{aligned} T'' - f'T' + 4f'T'(e^{-2f}T'^2 + 1) \\ = (T'^2 + e^{2f})\frac{\partial_T V(T)}{V(T)}, \end{aligned} \quad (2.13)$$

$$f'' - f'^2 + H^2 = -k_5^2 \frac{V(T)T'^2}{3\sqrt{e^{-2f}T'^2 + 1}}, \quad (2.14)$$

$$f'^2 - H^2 + \frac{k_5^2 e^{2f} \Lambda_5}{6} = -k_5^2 \frac{e^{2f} V(T)}{6\sqrt{e^{-2f}T'^2 + 1}}, \quad (2.15)$$

where  $H$  is constant.

After evaluating Eqs. (2.13), (2.14), and (2.15), the potential  $V(T)$  is explicitly obtained as [14–16]

$$V(T) = \begin{cases} -\Lambda_5 \operatorname{sech}\left[\sqrt{-\frac{2}{3}k_5^2 \Lambda_5 T}\right] \sqrt{6 \operatorname{sech}^2\left[\sqrt{-\frac{2}{3}k_5^2 \Lambda_5 T}\right] - 1} & (\Lambda_5 < 0) \\ \frac{3\sqrt{6}\sigma^2}{k_5^2} \operatorname{sec}\left[2 \operatorname{am}(i\sqrt{2}\sigma T, 2)\right] & (\Lambda_5 = 0, n = \frac{1}{2}), \\ -\Lambda_5 \operatorname{sec}\left[\sqrt{\frac{2}{3}k_5^2 \Lambda_5 T}\right] \sqrt{6 \operatorname{sec}^2\left[\sqrt{\frac{2}{3}k_5^2 \Lambda_5 T}\right] - 1} & (\Lambda_5 > 0) \end{cases} \quad (2.16)$$

where  $\sigma$  is constant, and Jacobi amplitude  $\operatorname{am}(u, l)$  is defined by

$$\phi = \operatorname{am}(u, l) = \int_0^u \operatorname{dn}(u', l) du'. \quad (2.17)$$

Here,  $\operatorname{dn}(u, l)$  is a Jacobi elliptic function with elliptic modulus. After taking  $k_5 = 1$  and  $\sigma = 1$ , with various values of the cosmological constant  $\Lambda_5$ , the potential  $V(T)$  as the function of the tachyon field  $T$  is depicted in Fig. 1.

### A. $\Lambda_5 < 0$ case

When we consider the five-dimensional gravity action with the negative cosmological constant  $\Lambda_5 < 0$ , after evaluating Eqs. (2.13), (2.14), and (2.15), the warped factor  $f(x)$  and the tachyon scalar field  $T(x)$  are obtained as

$$f(x) = \frac{1}{2} \ln\left[-\frac{6H^2 \operatorname{sech}[H(2x+\lambda)]}{k_5^2 \Lambda_5}\right], \quad (2.18)$$

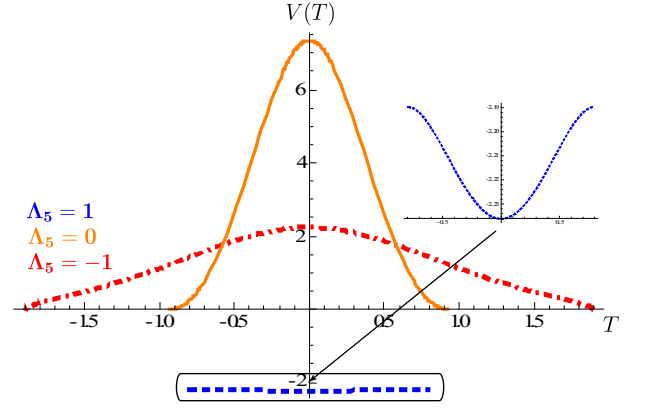


FIG. 1. Plot of potential  $V(T)$  as the function of the tachyon field  $T$  for  $k_5 = 1$  and  $\sigma = 1$  (red dotted-dashed curve for  $\Lambda_5 = -1$ , orange solid curve for  $\Lambda_5 = 0$ , blue dashed curve for  $\Lambda_5 = 1$ , respectively).

$$T(x) = \pm \sqrt{\frac{-3}{2k_5^2 \Lambda_5}} \tanh^{-1} \left[ \frac{\sinh\left[\frac{H(2x+\lambda)}{2}\right]}{\sqrt{\cosh[H(2x+\lambda)]}} \right], \quad (2.19)$$

and substituting into the potential  $V(T)$  (2.16), the potential  $V(x)$  is written as

$$V(x) = -\Lambda_5 \frac{\sqrt{3 \operatorname{sech}[H(2x+\lambda)] + 2} \sqrt{\operatorname{sech}[H(2x+\lambda)] + 1}}{\sqrt{2}}, \quad (2.20)$$

where  $\lambda$  is constant. The energy density  $\rho(x)$  is given as

$$\rho(x) = \frac{12H^2 (\cosh[H(2x+\lambda)] + 2)}{k_5^2 ((\cosh[2H(2x+\lambda)] + 1))}. \quad (2.21)$$

When  $\Lambda_5 = -1$ , shapes of potential  $V(x)$  as the function of the position  $x$  for various values of  $H$  are depicted in Fig. 2. The bigger  $H$  becomes, the more convex function in potential  $V(x)$ . Then, profiles of tachyon field  $T(x)$  for various  $H$  and profiles of energy density are depicted in Fig. 3 and Fig. 4, respectively. The five-dimensional curvature scalar  $\mathcal{R}$  is written as

$$\mathcal{R} = -\frac{14}{3} k_5^2 \Lambda_5 \operatorname{sech}[H(2x+\lambda)] \quad (2.22)$$

which is positive definite and asymptotically flat along the coordinate  $x$  as shown in Fig. 5. The configurational entropy of tachyon field  $S_{c, \text{AdS}}$  is numerically calculated by Eqs. (2.1), (2.2), and (2.4), and is depicted in Fig. 6. Especially,  $H$  increases, the configurational entropy reaches the minimum value ( $S_{c, \text{AdS}} = 0.0160325$ ) at a critical point ( $H_c = 1.61$ ).

In fact, the singular modes in momentum space broadly spread out and become plane waves with equally distributed modal. In addition through Fourier transforms, the corresponding modes in position space are sharply localized. The localized modes in position space have the maximum configurational entropy due to large amount of momentum modes whereas widespread modes in position space have the minimum configurational entropy due to small amount. Furthermore, configurational entropy is the portion of the entropy of a system that is given as the discrete representative positions of its constituent particles. For example, it may refer to the number of spin configurations in a magnet. As a given energy increases, its number increases. Thus, the smaller

configurational entropy of physical system becomes, the smaller its amount of energy to generate its configurations. The larger configurational entropy of physical system becomes, the larger its amount of energy to generate its configurations. Thus, one may expect that the predominant tachyonic states occurs at the minimum configurational entropy.

When the universe is accelerating expansion due to a negative pressure fluid, the simple example is that the universe with the scale factor  $a(t) = e^{Ht}$  is driven exponentially toward a flat geometry. Then the so-called horizon problem is solved by looking at the conformal time since accelerating expansion implies that the horizon size is shrinking in comoving units. Conformal time (comoving horizon) is defined as

$$\tau \equiv \int \frac{dt}{a(t)} = -\frac{1}{a(t)H}. \quad (2.23)$$

In particular, it seems that the constant  $H$  may be determined by the critical point  $H_c$ . The five-dimensional metric ansatz (2.24) on the brane reduces to the flat FRW metric via conformal time  $\tau$

$$ds_4^2 = a^2(\tau)(-d\tau^2 + d\alpha^2 + d\beta^2 + d\gamma^2), \quad (2.24)$$

where the constant warp factor  $e^{2f_0}$  is able to be absorbed by a rescaling of the spatial coordinates. For a radiation-dominated/matter-dominated universe the evolution of the scale factor  $a(\tau)$  in the metric (2.24) is obtained solving the Friedmann equations:

$$a(\tau) \propto \begin{cases} \tau = -\frac{1}{a(t)H} & \text{(RD),} \\ \tau^2 = \frac{1}{a^2(t)H^2} & \text{(MD)} \end{cases} \quad (2.25)$$

which seems to be determined by the above critical point  $H_c$ . Thus since the predominant tachyonic states occurs at  $H_c$ , it seems that accelerated rate of the universe and cosmological inflation rate for radiation/matter domination are able to be determined by such critical value.

### B. $\Lambda_5 = 0$ case

As discussed in the previous section we will apply a similar analysis to the five-dimensional gravity action without a bulk cosmological constant  $\Lambda_5$ .

The potential  $V(x)$  is obtained as [15]

$$V(x) = \frac{3\sqrt{\frac{2(n+1)}{n}}\sigma^{4n}}{k_5^2 H^{4n-2}} \text{sech}^{2(1-n)} \left[ H \left( \frac{x}{n} + \lambda \right) \right], \quad (2.26)$$

where  $\sigma$  is constant. The tachyon field  $T(x)$  is

$$T(x) = \pm \frac{\sqrt{\frac{n}{2(n-1)^2} {}_2F_1\left(\frac{1}{2}, \frac{1-n}{2}; \frac{3-n}{2}; \cosh\left[H\left(\frac{x}{n} + \lambda\right)\right]\right)}}{\sigma^{2n} H^{1-2n} \cosh^{n-1}\left[H\left(\frac{x}{n} + \lambda\right)\right]} + k, \quad (2.27)$$

where the hypergeometric function  ${}_2F_1(a, b; c; z)$  is defined for  $|z| > 1$  by the power series

$${}_2F_1(a, b; c; z) = \frac{\Gamma(b-a)\Gamma(c)(-z)^{-a}}{\Gamma(b)\Gamma(c-a)} \sum_{n=0}^{\infty} \frac{(a)_n (a-b+1)_n z^{-n}}{n!(a-b+1)_n} + \frac{\Gamma(a-b)\Gamma(c)(-z)^{-b}}{\Gamma(a)\Gamma(c-b)} \sum_{n=0}^{\infty} \frac{(b)_n (b-c+1)_n z^{-n}}{n!(b-a+1)_n} \quad (2.28)$$

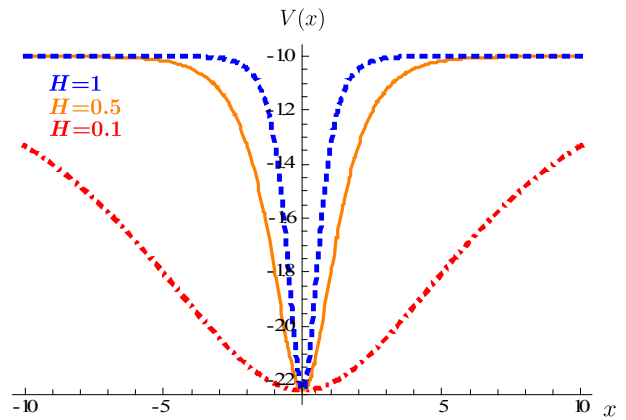


FIG. 2. Plot of potential  $V(x)$  as the function of the position  $x$  for  $k_5 = 1$ ,  $\Lambda_5 = -1$ , and  $\lambda = 0$  (red dotted-dashed curve for  $H = 0.1$ , orange solid curve for  $H = 0.5$ , blue dashed curve for  $H = 1$ , respectively).

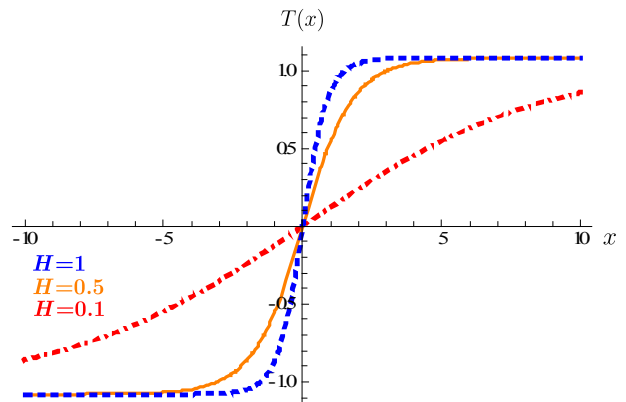


FIG. 3. Plot of the tachyon field  $T(x)$  as the function of the position  $x$  for  $k_5 = 1$ ,  $\Lambda_5 = -1$ , and  $\lambda = 0$  (red dotted-dashed curve for  $H = 0.1$ , orange solid curve for  $H = 0.5$ , blue dashed curve for  $H = 1$ , respectively).

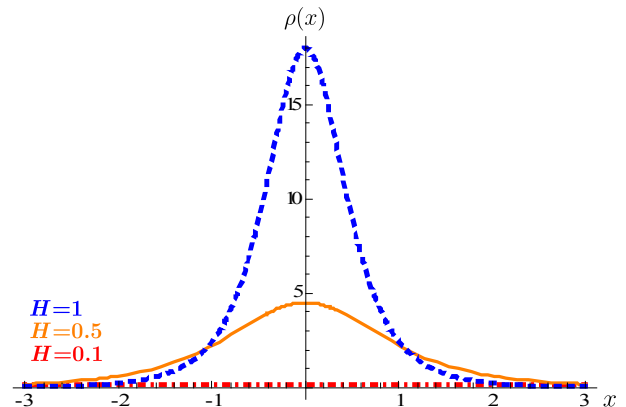


FIG. 4. Plot of energy density  $\rho(x)$  as the function of the position  $x$  for  $k_5 = 1$ ,  $\Lambda_5 = -1$ , and  $\lambda = 0$  (red dotted-dashed curve for  $H = 0.1$ , orange solid curve for  $H = 0.5$ , blue dashed curve for  $H = 1$ , respectively).

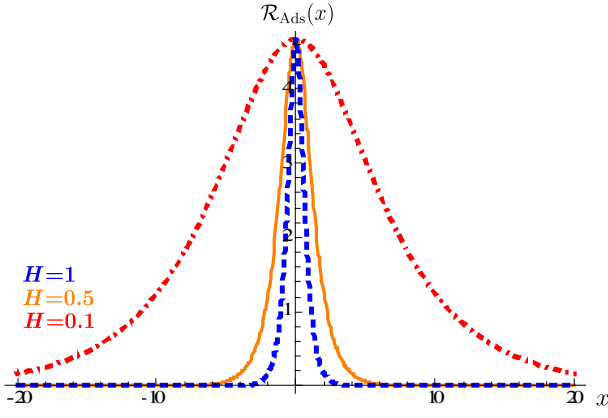


FIG. 5. Plot of curvature scalar  $\mathcal{R}_{\text{AdS}}(x)$  as the function of the position  $x$  for  $k_5 = 1$ ,  $\Lambda_5 = -1$ , and  $\lambda = 0$  (red dotted-dashed curve for  $H = 0.1$ , orange solid curve for  $H = 0.5$ , blue dashed curve for  $H = 1$ , respectively).

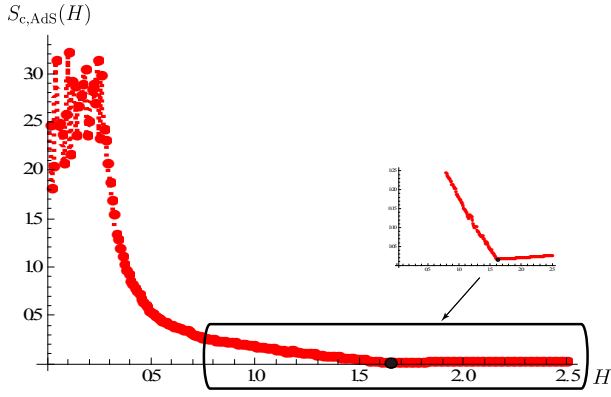


FIG. 6. Plot of tachyon configurational entropy  $S_{c,\text{AdS}}$  as the function of  $H$  for  $k_5 = 1$ ,  $\Lambda_5 = -1$ , and  $\lambda = 1$ .

and  $a - b$  must not be an integer. Here, for  $0 < n < 1$  the tachyon field becomes real value by introducing a complex constant  $l$ . The warped factor  $f(x)$  is [15]

$$f(x) = -n \ln \left[ \frac{\sigma^2 \cosh(H(\frac{x}{n} + \lambda))}{H^2} \right]. \quad (2.29)$$

For  $n = 1/2$ , the potential  $V(x)$  (2.26) is obtained as

$$V(x) = \frac{3\sqrt{6}\sigma^2}{k_5^2} \text{sech}[H(2x + \lambda)], \quad (2.30)$$

the tachyon field  $T(x)$  (2.27) leads to

$$T(x) = \pm \frac{1}{\sqrt{2}\sigma} F \left[ iH \left( x + \frac{\lambda}{2} \right), 2 \right], \quad (2.31)$$

where for  $-\pi/2 < \phi < \pi/2$ , the elliptic integral of the first kind  $F(\phi, \kappa)$  is defined by

$$F(\phi, \kappa) = \int_0^\phi \frac{1}{\sqrt{1 - \kappa^2 \sin^2(\theta)}} d\theta. \quad (2.32)$$

For  $n = 1/2$ , the warped factor  $f(x)$  (2.29) is given as

$$f(x) = -\frac{1}{2} \ln \left[ \frac{\sigma^2 \cosh[H(2x + \lambda)]}{H^2} \right]. \quad (2.33)$$

Then, the energy density  $\rho$ , and the five-dimensional curvature scalar  $\mathcal{R}$  are

$$\rho(x) = \frac{6\sqrt{6}H^2}{k_5^2 (\cosh[2H(2x + \lambda)] + 1)}, \quad (2.34)$$

$$\mathcal{R} = 28\sigma^2 \text{sech}[H(2x + \lambda)]. \quad (2.35)$$

When  $\Lambda_5 = 0$  and  $n = 1/2$ , shapes of potential  $V(x)$  as the function of the position  $x$  for various values of  $H$  are depicted in Fig. 7. The smaller  $H$  becomes, the more convex function in potential  $V(x)$ . Then, profiles of tachyon field  $T(x)$  for various  $H$  and profiles of energy density are depicted in Fig. 8 and Fig. 9. The five-dimensional curvature scalar  $\mathcal{R}$  is depicted in Fig. 10. The configurational entropy of tachyon field  $S_{c,\text{Flat}}$  is numerically calculated by Eqs. (2.1), (2.2), and (2.4), and is depicted in Fig. 11. Especially,  $H$  grows up, the configurational entropy reaches the minimum value ( $S_{c,\text{Flat}} = 0.013826$ ) at a critical point ( $H_c = 1.26$ ). Thus, as discussed in the previous AdS case, it is expected that the predominant tachyonic states happens at the minimum configurational entropy.

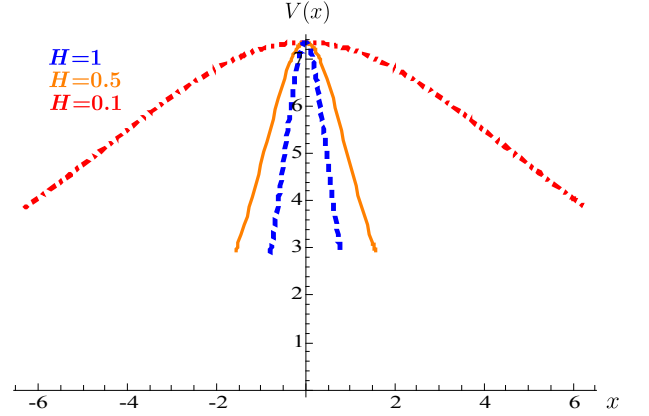


FIG. 7. Plot of potential  $V(x)$  as the function of the position  $x$  for  $k_5 = 1$ ,  $n = 1/2$ ,  $\sigma = 1$  and  $\lambda = 0$  (red dotted-dashed curve for  $H = 0.1$ , orange solid curve for  $H = 0.5$ , blue dashed curve for  $H = 1$ , respectively).

### C. $\Lambda_5 > 0$ case

In the case of the five-dimensional gravity action with the positive cosmological constant  $\Lambda_5 > 0$ , the potential  $V(x)$ , the tachyon field  $T$ , the warped factor  $f(x)$ , the energy density  $\rho(x)$ , and the five-dimensional curvature scalar  $\mathcal{R}$  are obtained as

$$V(x) = -\Lambda_5 \frac{\sqrt{3 \sec[H(2x + \lambda)] + 2} \sqrt{\sec[H(2x + \lambda)] + 1}}{\sqrt{2}}, \quad (2.36)$$

$$T(x) = \pm \sqrt{\frac{3}{2k_5^2 \Lambda_5}} \tanh^{-1} \left[ \frac{\sin(\frac{H(2x + \lambda)}{2})}{\sqrt{\cos(H(2x + \lambda))}} \right], \quad (2.37)$$

$$f(x) = \frac{1}{2} \ln \left[ \frac{6H^2 \sec[H(2x + \lambda)]}{k_5^2 \Lambda_5} \right], \quad (2.38)$$

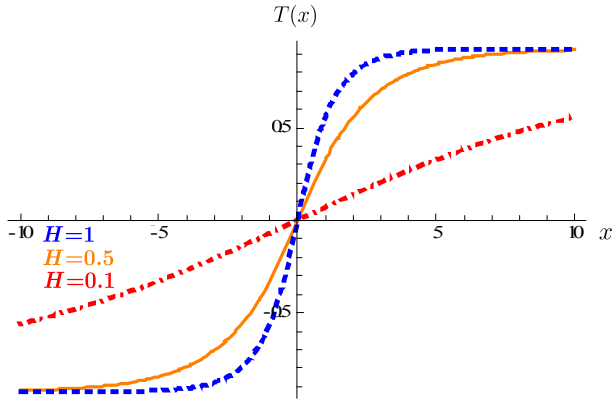


FIG. 8. Plot of the tachyon field  $T(x)$  as the function of the position  $x$  for  $n = 1/2$ ,  $\sigma = 1$  and  $\lambda = 0$  (red dotted-dashed curve for  $H = 0.1$ , orange solid curve for  $H = 0.5$ , blue dashed curve for  $H = 1$ , respectively).

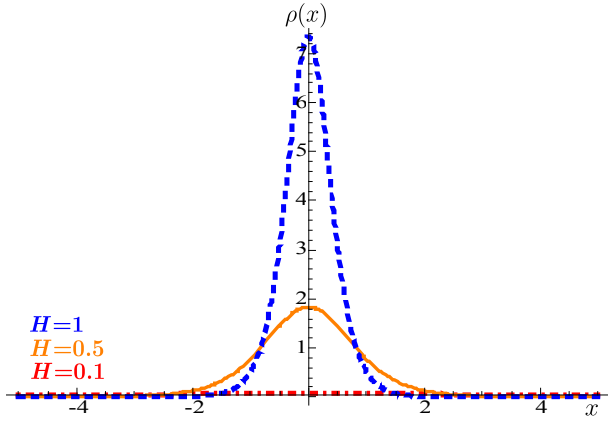


FIG. 9. Plot of energy density  $\rho(x)$  as the function of the position  $x$  for  $k_5 = 1$ ,  $n = 1/2$ ,  $\sigma = 1$  and  $\lambda = 0$  (red dotted-dashed curve for  $H = 0.1$ , orange solid curve for  $H = 0.5$ , blue dashed curve for  $H = 1$ , respectively).

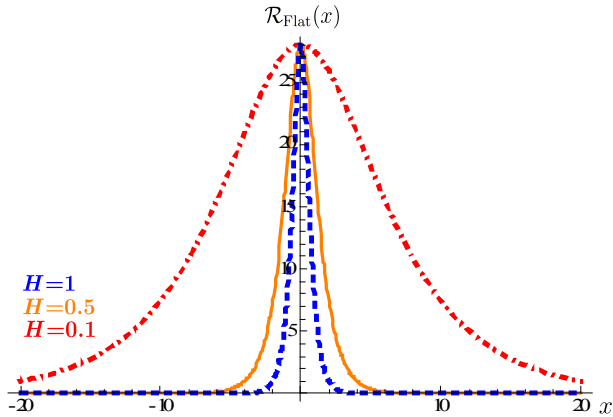


FIG. 10. Plot of curvature scalar  $\mathcal{R}_{\text{Flat}}(x)$  as the function of the position  $x$  for  $n = 1/2$ ,  $\sigma = 1$  and  $\lambda = 0$  (red dotted-dashed curve for  $H = 0.1$ , orange solid curve for  $H = 0.5$ , blue dashed curve for  $H = 1$ , respectively).

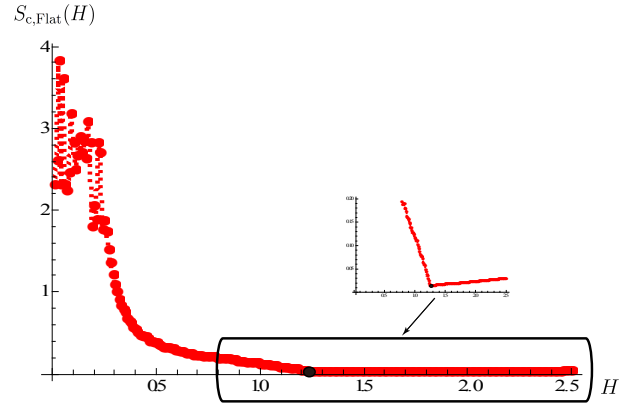


FIG. 11. Plot of tachyon configurational entropy  $S_{c,\text{Flat}}$  as the function of  $H$  for  $k_5 = 1$ ,  $n = 1/2$ ,  $\sigma = 1$  and  $\lambda = 1$ .

$$\rho(x) = \frac{6H^2 \sqrt{\sec[H(2x+\lambda)+1]} \sqrt{3 \sec[H(2x+\lambda)+2]}}{k_5^2 (\cos[H(2x+\lambda)]+1) \sqrt{2-1/(\cos[H(2x+\lambda)]+1)}} \quad (2.39)$$

$$\mathcal{R} = \frac{14}{3} k_5^2 \Lambda_5 \sec[H(2x + \lambda)]. \quad (2.40)$$

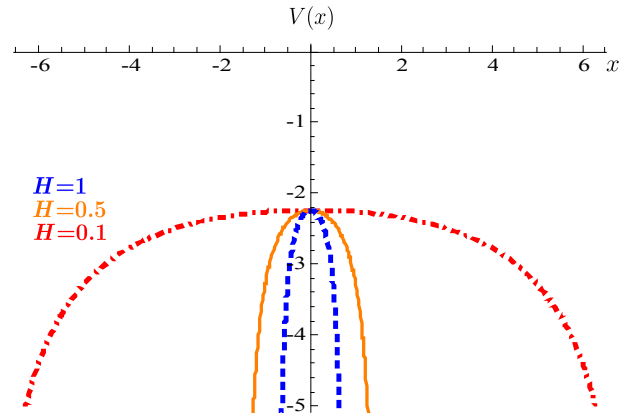


FIG. 12. Plot of potential  $V(x)$  as the function of the position  $x$  for  $k_5 = 1$ ,  $\Lambda_5 = 1$ , and  $\lambda = 0$  (red dotted-dashed curve for  $H = 0.1$ , orange solid curve for  $H = 0.5$ , blue dashed curve for  $H = 1$ , respectively).

When  $\Lambda_5 > 0$ , shapes of potential  $V(x)$  as the function of the position  $x$  for various values of  $H$  are depicted in Fig. 12. The bigger  $H$  becomes, the more convex function in potential  $V(x)$ . Then, profiles of tachyon field  $T(x)$  for various  $H$  and profiles of energy density are depicted in Fig. 13 and Fig. 14, respectively. The five-dimensional curvature scalar  $\mathcal{R}$  is depicted in Fig. 15. The configurational entropy of tachyon field  $S_{c,\text{dS}}$  is numerically calculated by Eqs. (2.1), (2.2), and (2.4), and is depicted in Fig. 16. As  $H$  grows up,  $S_{c,\text{dS}}$  almost monotonically decreases, which contrasts with the results in Fig. 6 and Fig. 11. Here, it seems that the local minimum configurational entropy is absent.

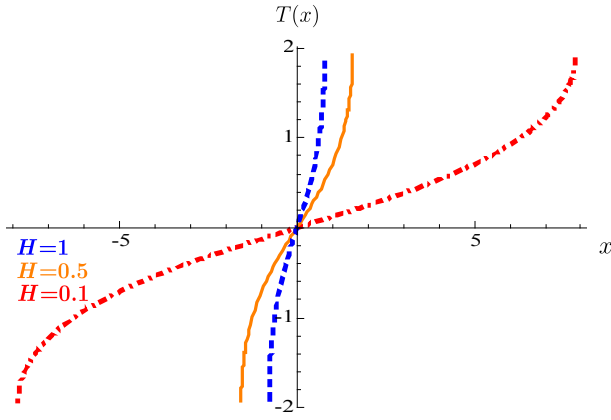


FIG. 13. Plot of the tachyon field  $T(x)$  as the function of the position  $x$  for  $k_5 = 1$ ,  $\Lambda_5 = 1$ , and  $\lambda = 0$  (red dotted-dashed curve for  $H = 0.1$ , orange solid curve for  $H = 0.5$ , blue dashed curve for  $H = 1$ , respectively).

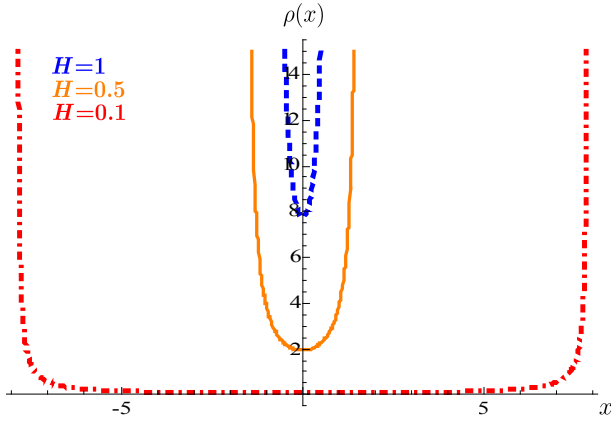


FIG. 14. Plot of energy density  $\rho(x)$  as the function of the position  $x$  for  $k_5 = 1$ ,  $\Lambda_5 = 1$ , and  $\lambda = 0$  (red dotted-dashed curve for  $H = 0.1$ , orange solid curve for  $H = 0.5$ , blue dashed curve for  $H = 1$ , respectively).

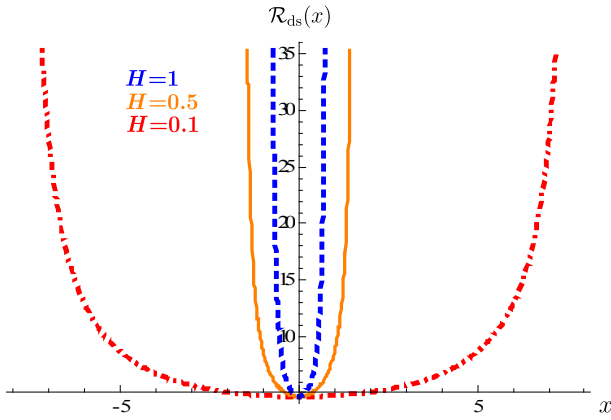


FIG. 15. Plot of curvature scalar  $\mathcal{R}_{ds}(x)$  as the function of the position  $x$  for  $k_5 = 1$ ,  $\Lambda_5 = 1$ , and  $\lambda = 0$  (red dotted-dashed curve for  $H = 0.1$ , orange solid curve for  $H = 0.5$ , blue dashed curve for  $H = 1$ , respectively).

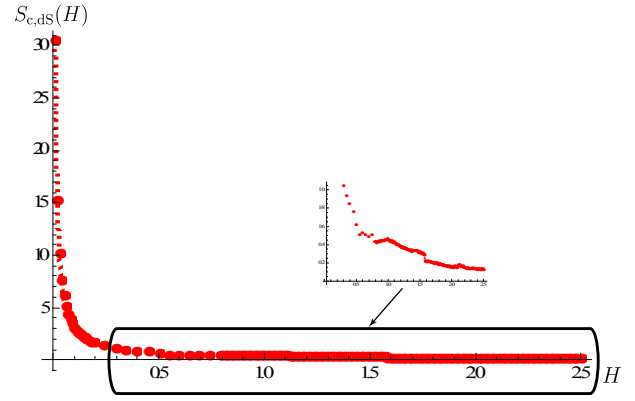


FIG. 16. Plot of tachyon configurational entropy  $S_{c,ds}$  as the function of  $H$  for  $k_5^2 = 1$ ,  $\Lambda_5 = 1$ , and  $\lambda = 1$ .

### III. INSTABILITY OF TACHYONIC BRANEWORLD

In this section, employing superpotential operators via supersymmetric quantum mechanics, we will investigate instability of tachyonic braneworld model under scalar fluctuations [16, 29–31].

The respective fluctuations of tachyonic braneworld model under scalar perturbations are given as the following equations [14, 16]

$$\delta \square T - \delta \left( \frac{\nabla_\mu \nabla_\nu T \nabla^\mu T \nabla^\nu T}{1 + g^{\mu\nu} \nabla_\mu T \nabla_\nu T} \right) = \delta \left( \frac{\partial_T V}{V} \right), \quad (3.1)$$

$$\delta R_\mu^\nu - \frac{1}{2} \delta_\mu^\nu \delta R = k_5^2 \delta T_\mu^\nu. \quad (3.2)$$

Employing  $\varphi(T) = \varphi_0(T) + \delta\varphi(T)$  and considering the scalar sector of the 5D perturbed metric

$$ds_5^2 = e^{2f} [(1 + 2\phi)dx^2 + (1 + 2\psi)\gamma_{cd}d\alpha^c d\alpha^d], \quad (3.3)$$

the perturbed bulk energy-momentum tensor of the tachyonic fields is given as

$$\begin{aligned} \delta T_\mu^\nu = & - \left[ \frac{\sqrt{1+e^{-2f}\varphi_0'^2}(\partial_{\varphi_0}V)\delta\varphi + \frac{e^{-2f}\varphi_0'V(\delta\varphi' - \phi\varphi_0')}{\sqrt{1+e^{-2f}\varphi_0'^2}}}{\sqrt{1+e^{-2f}\varphi_0'^2}} \right] \delta_\mu^\nu \\ & + e^{-2f}\varphi_0'^2 \left[ \frac{(\partial_{\varphi_0}V)\delta\varphi}{\sqrt{1+e^{-2f}\varphi_0'^2}} - \frac{e^{-2f}\varphi_0'V(\delta\varphi' - \phi\varphi_0')}{(1+e^{-2f}\varphi_0'^2)^{3/2}} \right] \delta_\mu^\nu \delta_\nu^\nu \\ & + \frac{\varphi_0'V}{\sqrt{1+e^{-2f}\varphi_0'^2}} [\delta_\mu^\nu \partial^\nu \delta\varphi + e^{-2f}(\delta_\mu^\nu \partial_\mu \delta\varphi - 2\delta_\mu^\nu \delta_\nu^\nu \phi\varphi_0')] \end{aligned} \quad (3.4)$$

Here, the small Roman indices ( $c, d = 0, 1, 2, 3$ ) denote the spacetime indices of the braneworlds.

The generalized definition of the 4D mass space-times with constant curvature is defined as [16, 29–31]

$$\gamma^{cd} \nabla_c \nabla_d - 2H^2 \equiv m^2, \quad (3.5)$$

where the Hubble parameter  $H$  is connected to the spatial curvature  $K$  as follows  $H^2 = K$ . After some algebra, one can get the following equation

$$\begin{aligned} & (A-1)\psi'' + [f' - D + B(A-2)]\psi' + 2[2f'' - 2f'^2 - f'D + C(A-2) - 2K]\psi \\ & = (\gamma^{cd} \nabla_c \nabla_d - 2K)\psi \equiv m^2 \psi \end{aligned} \quad (3.6)$$

where the functions  $A(x)$ ,  $B(x)$ ,  $C(x)$ ,  $D(x)$ ,  $F(x)$  are given as  $A = \frac{e^{-2f}\varphi_0'^2}{1+e^{-2f}\varphi_0'^2}$ ,  $B = \frac{F'}{F} + 2f'$ ,  $C = \frac{F'}{F}f' + f'' + \frac{\varphi_0'}{F}$ ,  $D = \frac{\varphi_0'}{V}\partial_{\varphi_0}V$ ,  $F = -\frac{3\sqrt{1+e^{-2f}\varphi_0'^2}}{k_5^2\varphi_0'V}$ , which leads to a Schrödinger-like form

$$-(1-A)G'' + \mathcal{V}G = m^2G, \quad (3.7)$$

through the following transformation  $\psi = \frac{G(x, \alpha^c)}{\sqrt{\xi(x)}}$ . Here the associated potential  $\mathcal{V}$  is given as

$$\mathcal{V} = \frac{7}{2}f'' - 4f'^2 - \frac{1}{2}\eta_1' + 2\eta_2 - 4K - \frac{[\frac{1}{2}f'^2 + \frac{1}{2}\eta_1' + f'\eta_1 - A'(f' + \eta_1)]}{2(A-1)}, \quad (3.8)$$

with  $\eta_1 = -D + B(A-2)$  and  $\eta_2 = -f'D + C(A-2) - 4K$ . The potential  $\mathcal{V}(x)$  is related to the superpotential  $\mathcal{J}(x)$

$$\mathcal{V} = \mathcal{J}^2 - \sqrt{1-A}\mathcal{J}' - \frac{1}{4}A'' - \frac{3}{16}\frac{A'^2}{1-A}, \quad (3.9)$$

and the supersymmetric operators  $\Pi^\dagger$  and  $\Pi$  are obtained as

$$\Pi^\dagger = \left( -\sqrt{1-A}\frac{\partial}{\partial x} - \frac{1}{4}\frac{A'}{\sqrt{1-A}} + \mathcal{J} \right), \quad (3.10)$$

$$\Pi = \left( \sqrt{1-A}\frac{\partial}{\partial x} + \frac{1}{4}\frac{A'}{\sqrt{1-A}} + \mathcal{J} \right), \quad (3.11)$$

which leads to

$$\begin{aligned} \Pi^\dagger \Pi F &= -(1-A)F'' + \left( -\frac{1}{4}A'' - \frac{3}{16}\frac{A'^2}{1-A} + \mathcal{J}^2 - \sqrt{1-A}\mathcal{J}' \right) F \\ &= m^2 F. \end{aligned} \quad (3.12)$$

Once the Schrodinger-like equation can be written in terms of the supersymmetric operators  $\Pi^\dagger$  and  $\Pi$ , there are no states with usable modes, which is borrowed from supersymmetric quantum mechanics [16, 29–31]. Employing the auxiliary field  $\mathcal{X}$ , the superpotential  $\mathcal{J}$  may be defined as

$$\mathcal{J} = \sqrt{1-A} \left( \frac{A'}{1-A} - \frac{\mathcal{X}'}{\mathcal{X}} \right) \quad (3.13)$$

After some algebra, Eq. (3.12) reduces to

$$\mathcal{X}'' + \mathcal{Y}\mathcal{X} = 0, \quad (3.14)$$

where the function  $\mathcal{Y}$  is given as

$$\mathcal{Y} = \frac{1}{A-1} \left( A'' + \frac{2}{A-1}(\zeta_1 - A'^2) + \zeta_2 \right), \quad (3.15)$$

with  $\zeta_1 = A'^2 + (A-1)A'\frac{\mathcal{X}'}{\mathcal{X}}$  and  $\zeta_2 = -A'' - 2A'\frac{\mathcal{X}'}{\mathcal{X}} - (A-1)\frac{\mathcal{X}''}{\mathcal{X}}$ . Furthermore, since the tachyon field in the action (2.5) is real,  $\sqrt{1-A}$  in the supersymmetric operators (3.10) and (3.11) must be real, which applies for

solutions of tachyonic braneworld in the bulk dS space. This results in the following relations

$$1-A = \begin{cases} \frac{6H^2}{6H^2 - k_5^2 \Lambda_5 \cosh[H(2x+\lambda)]\varphi_0^2} & (\Lambda_5 < 0) \\ \frac{H^2}{H^2 + \sigma^2 \cosh[H(2x+\lambda)]\varphi_0^2} & (\Lambda_5 = 0, n = \frac{1}{2}). \\ \frac{6H^2}{6H^2 + k_5^2 \Lambda_5 \cos[H(2x+\lambda)]\varphi_0^2} & (\Lambda_5 > 0) \end{cases} \quad (3.16)$$

When  $\Lambda_5 < 0$ , since  $1 \leq \cosh[H(2x+\lambda)] \leq \infty$ , the range of  $1-A$  is given as  $0 \leq 1-A \leq \frac{6H^2}{6H^2 - k_5^2 \Lambda_5 \varphi_0^2}$ , which is always positive definite. For example, (i) taking  $H = \frac{1}{\sqrt{2}}$ ,  $k_5 = \sqrt{6}$ ,  $\Lambda_5 = -1$ ,  $\lambda = 0$ , and  $\varphi_0 = 1$ ,  $1-A$  is given as  $\frac{1}{1+2\cosh(\sqrt{2}x)}$  (see red dotted-dashed curve in Fig. 17). (ii) taking  $H = 1$ ,  $k_5 = \sqrt{6}$ ,  $\Lambda_5 = -1$ ,  $\lambda = 0$ , and  $\varphi_0 = 1$ ,  $1-A$  is  $\frac{1}{2\cosh^2(x)}$  (see orange solid curve in Fig. 17). (iii) taking  $H = \sqrt{10}$ ,  $k_5 = \sqrt{6}$ ,  $\Lambda_5 = -1$ ,  $\lambda = 0$ , and  $\varphi_0 = 1$ ,  $1-A$  is  $\frac{10}{10+\cosh(2\sqrt{10}x)}$  (blue dashed curve in Fig. 17). The magnitude of  $1-A$  is depicted in Fig. 17, and is positive in any case. The tachyon braneworld in the bulk AdS space is stable under scalar fluctuations, which is consistent with that in [14, 16].

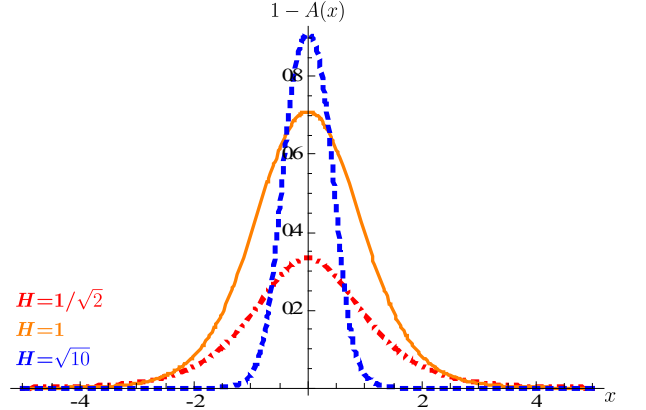


FIG. 17. Plot of the magnitude of  $1-A$  as the function of the position  $x$  for  $k_5 = \sqrt{6}$ ,  $\Lambda_5 = -1$ ,  $\lambda = 0$ , and  $\varphi_0 = 1$  (red dotted-dashed curve for  $H = 1/\sqrt{2}$ , orange solid curve for  $H = 1$ , blue dashed curve for  $H = \sqrt{10}$ , respectively).

When  $\Lambda_5 = 0$ ,  $H$  and  $\sigma$  of  $1-A$  are replaced by  $6H$  and  $-k_5^2\Lambda_5$  respectively, which reduces to  $1-A$  in the above bulk AdS case. Thus, the tachyon braneworld model without the bulk cosmological constant is also stable under scalar fluctuations, which is consistent with that in [15].

Finally, when  $\Lambda_5 > 0$ , since  $-1 \leq \cos[H(2x+\lambda)] \leq 1$ , the magnitude of  $1-A$  becomes positive for  $6H^2 > k_5^2\Lambda_5\varphi_0^2$ . For example, (i) taking  $H = \frac{1}{\sqrt{2}}$ ,  $k_5 = \sqrt{6}$ ,  $\Lambda_5 = 1$ ,  $\lambda = 0$ , and  $\varphi_0 = 1$ , in the case of  $[(6H^2 = 3) < (k_5^2\Lambda_5\varphi_0^2 = 6)]$ ,  $1-A$  is given as  $\frac{1}{1+2\cos(\sqrt{2}x)}$ . The value of the function is positive for  $\frac{\sqrt{2}(3n-1)\pi}{3} < x < \frac{\sqrt{2}(3n+1)\pi}{3}$  whereas it is negative for  $\frac{\sqrt{2}(3n+1)\pi}{3} < x < \frac{\sqrt{2}(3n+2)\pi}{3}$ .

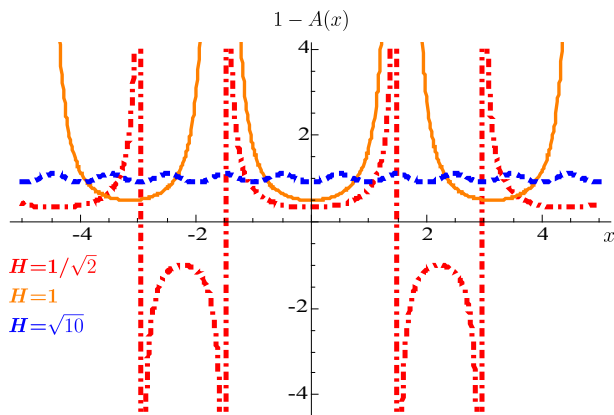


FIG. 18. Plot of the magnitude of  $1 - A$  as the function of the position  $x$  for  $k_5 = \sqrt{6}$ ,  $\Lambda_5 = 1$ ,  $\lambda = 0$ , and  $\varphi_0 = 1$  (red dotted-dashed curve for  $H = 1/\sqrt{2}$ , orange solid curve for  $H = 1$ , blue dashed curve for  $H = \sqrt{10}$ , respectively).

where  $n$  is a integer value (see red dotted-dashed curve in Fig. 18). (ii) taking  $H = 1$ ,  $k_5 = \sqrt{6}$ ,  $\Lambda_5 = 1$ ,  $\lambda = 0$ , and  $\varphi_0 = 1$ , in the case of  $[(6H^2 = 6) = (k_5^2 \Lambda_5 \varphi_0^2 = 6)]$ ,  $1 - A$  is  $\frac{1}{2 \cos^2(x)}$ , which is positive but is singular at some points ( $x = n\pi$ ) (see orange solid curve in Fig. 18). (iii) taking  $H = \sqrt{10}$ ,  $k_5 = \sqrt{6}$ ,  $\Lambda_5 = 1$ ,  $\lambda = 0$ , and  $\varphi_0 = 1$ , in the case of  $[(6H^2 = 60) > (k_5^2 \Lambda_5 \varphi_0^2 = 6)]$ ,  $1 - A$  is  $\frac{10}{10 + \cos(2\sqrt{10}x)}$  and is always positive (blue dashed curve in Fig. 18). It implies that the tachyon braneworld in the bulk dS space is stable under scalar fluctuations when  $6H^2 > k_5^2 \Lambda_5 \varphi_0^2$ .

## IV. CONCLUSION

We considered the tachyonic system coupled to gravity with the bulk cosmological constant and investigated its configurational entropy. For  $\Lambda_5 < 0$  or  $\Lambda_5 = 0$ , we found that the configurational entropy becomes a global minimum as the magnitude of scale factor reaches the critical value. It seems that an accelerated rate of the universe and cosmological inflation rate for radiation/matter domination can be determined by such critical value. For  $\Lambda_5 > 0$ , we also found that an exact solution of the tachyonic braneworld, and the configurational entropy monotonically decreases when increasing the magnitude of scale factor.

Employing the replacement of the supersymmetric operators by the specific solution of the field equations, we found that tachyon braneworld in the bulk negative/zero cosmological constant is stable under scalar fluctuations, which is consistent with that in [14–16]. We applied similar analysis to the instability of tachyonic braneworld model in the bulk positive cosmological constant. It was shown that such model is stable under scalar fluctuations when  $6H^2 > k_5^2 \Lambda_5 \varphi_0^2$ .

## ACKNOWLEDGEMENTS

This work was supported by Basic Science Research Program through the National Research Foundation of Korea (NRF) funded by the Ministry of Education, Science and Technology (NRF-2018R1D1A1B07049451).

- 
- [1] A. Sen, JHEP **9808**, 012 (1998) [hep-th/9805170].
  - [2] A. Sen, JHEP **0204**, 048 (2002) [hep-th/0203211].
  - [3] A. Sen, JHEP **0207**, 065 (2002) [hep-th/0203265].
  - [4] A. Sen, Mod. Phys. Lett. A **17**, 1797 (2002) [hep-th/0204143].
  - [5] J. M. Cline, H. Firouzjahi and P. Martineau, JHEP **0211**, 041 (2002) [hep-th/0207156].
  - [6] G. N. Felder, L. Kofman and A. Starobinsky, JHEP **0209**, 026 (2002) [hep-th/0208019].
  - [7] G. N. Felder and L. Kofman, Phys. Rev. D **70**, 046004 (2004) [hep-th/0403073].
  - [8] N. Barnaby, JHEP **0407**, 025 (2004) [hep-th/0406120].
  - [9] N. D. Lambert, H. Liu and J. M. Maldacena, JHEP **0703**, 014 (2007) [hep-th/0303139].
  - [10] J. Kluson, JHEP **0401**, 019 (2004) [hep-th/0312086].
  - [11] C. j. Kim, Y. b. Kim and C. O. Lee, JHEP **0305**, 020 (2003) [hep-th/0304180].
  - [12] C. Kim, Y. Kim, O. K. Kwon and C. O. Lee, JHEP **0311**, 034 (2003) [hep-th/0305092].
  - [13] A. Sen, Phys. Rev. D **68**, 106003 (2003) [hep-th/0305011].
  - [14] G. German, A. Herrera-Aguilar, D. Malagon-Morejon, R. R. Mora-Luna and R. da Rocha, JCAP **1302**, 035 (2013) [arXiv:1210.0721 [hep-th]].
  - [15] N. Barbosa-Cendejas, R. Cartas-Fuentevilla, A. Herrera-Aguilar, R. R. Mora-Luna and R. da Rocha, JCAP **1801**, no. 01, 005 (2018) doi:10.1088/1475-7516/2018/01/005 [arXiv:1709.09016 [hep-th]].
  - [16] G. German, A. Herrera-Aguilar, A. M. Kuerten, D. Malagon-Morejon and R. da Rocha, JCAP **1601**, no. 01, 047 (2016) doi:10.1088/1475-7516/2016/01/047 [arXiv:1508.03867 [hep-th]].
  - [17] M. Gleiser and N. Stamatopoulos, Phys. Lett. B **713**, 304 (2012) [arXiv:1111.5597 [hep-th]].
  - [18] M. Gleiser and N. Stamatopoulos, Phys. Rev. D **86**, 045004 (2012) [arXiv:1205.3061 [hep-th]].
  - [19] A. E. Bernardini and R. da Rocha, Phys. Lett. B **762**, 107 (2016) [arXiv:1605.00294 [hep-th]].
  - [20] A. E. Bernardini, N. R. F. Braga and R. da Rocha, Phys. Lett. B **765**, 81 (2017) [arXiv:1609.01258 [hep-th]].
  - [21] M. Gleiser and D. Sowinski, Phys. Lett. B **727**, 272 (2013) [arXiv:1307.0530 [hep-th]].
  - [22] M. Gleiser and N. Graham, Phys. Rev. D **89**, no. 8, 083502 (2014) [arXiv:1401.6225 [astro-ph.CO]].
  - [23] M. Gleiser and N. Jiang, Phys. Rev. D **92**, no. 4, 044046 (2015) [arXiv:1506.05722 [gr-qc]].
  - [24] R. Casadio and R. da Rocha, Phys. Lett. B **763**, 434 (2016) [arXiv:1610.01572 [hep-th]].



- [25] N. R. F. Braga and R. da Rocha, *Phys. Lett. B* **767** (2017) 386 [arXiv:1612.03289 [hep-th]].
- [26] C. O. Lee, *Phys. Lett. B* **772**, 471 (2017) [arXiv:1705.09047 [gr-qc]].
- [27] M. Gleiser, M. Stephens and D. Sowinski, *Phys. Rev. D* **97**, no. 9, 096007 (2018) [arXiv:1803.08550 [hep-th]].
- [28] C. O. Lee, *Phys. Lett. B* **790**, 197 (2019) doi:10.1016/j.physletb.2019.01.026 [arXiv:1812.00343 [gr-qc]].
- [29] M. Giovannini, *Phys. Rev. D* **64**, 064023 (2001) doi:10.1103/PhysRevD.64.064023 [hep-th/0106041].
- [30] S. Kobayashi, K. Koyama and J. Soda, *Phys. Rev. D* **65**, 064014 (2002) doi:10.1103/PhysRevD.65.064014 [hep-th/0107025].
- [31] M. Giovannini, *Class. Quant. Grav.* **20**, 1063 (2003) doi:10.1088/0264-9381/20/6/303 [gr-qc/0207116].